Bulletin of the Seismological Society of America, Vol. 77, No. 2, pp. 440–467, April 1987

STOCHASTIC PREDICTION OF GROUND MOTION AND SPECTRAL RESPONSE PARAMETERS AT HARD-ROCK SITES IN EASTERN NORTH AMERICA

BY DAVID M. BOORE AND GAIL M. ATKINSON*

ABSTRACT

Empirical predictions of ground motions from large eastern North American earthquakes are hampered by a lack of data for such events. For this reason, most prediction techniques have been based, at least in part, on data from the seismically active and well-instrumented western North America. Concentrating on the prediction of response spectra on hard-rock sites, we have used a relatively new, theoretical technique that does not require western data to make ground motion predictions for eastern North America. This method, often referred to as the stochastic model, has its origins in the work of Hanks and McGuire, who treat high-frequency motions as filtered random Gaussian noise, for which the filter parameters are determined by a seismological model of both the source and the wave propagation. The model has been successfully applied to the predictions of ground motions in the Western United States and to short-period magnitudes from large to great earthquakes worldwide. For our application, the essential parameters of the model are estimated by using existing data from small to moderate eastern North American earthquakes. A crucial part of the model is the relation between seismic moment and corner frequency. The relation proposed in 1983 by Nuttli for mid-plate earthquakes leads to predictions of ground motions that are lower than available data by a factor of about 4. On the other hand, a constant stress parameter of 100 bars gives model predictions in good accord with the data. To aid in applications, the ground motion predictions are given in the form of regression equations for earthquakes of magnitude 4.5 to 7.5, at distances within 100 km of the source. The explanatory variables are hypocentral distance and moment magnitude (M). Because predictions are often required in terms of m_{Lg} rather than M, we have used the theoretical model to establish a relation between the two magnitudes. The predicted relation agrees with the sparse data available, although the large uncertainties in the observed magnitudes for the larger events, as well as the sensitivity of the theoretical magnitude to the attenuation model, make it difficult to discriminate between various source-scaling models.

INTRODUCTION

The prediction of ground motion or response amplitude as a function of earthquake magnitude and distance is of fundamental importance to the assessment of seismic hazard. Historically, attenuation relations were first developed empirically for California by regression analysis of observed ground motion parameters, most typically peak horizontal acceleration ($a_{\max}$). Recent relations of this genre (Joyner and Boore, 1981; Campbell, 1981) are quite reliable for California, where there is now a good strong-motion data base, albeit with significant shortcomings for large magnitudes at near distances. For eastern North America (ENA), the lack of a strong-motion data base necessitated the development of prediction relations by indirect methods. Typically, correlations of Modified Mercalli Intensity (MMI) with $a_{\max}$, and possibly distance, were combined with observations on the attenuation of

* Present address: 125 Dunbar Road South, Waterloo, Ontario, Canada.

MMI to derive a_{max} attenuation (e.g., Milne and Davenport, 1969; Hasegawa *et al.*, 1981; McGuire, 1984). Alternatively, eastern ground motions were assumed comparable to western motions for the same magnitude near the source, but were attenuated more slowly, to account for the slow attenuation of the *Lg* phase in ENA (Campbell, 1982). Nuttli and Herrmann (1978) and Herrmann and Nuttli (1984) used a semi-theoretical method in which theoretical scaling with magnitude was constrained by the limited ground motion data (most of which are for earthquakes with magnitudes around 5).

Another way of deriving prediction equations, similar in spirit to Herrmann and Nuttli, is to use stochastic methods in conjunction with a theoretical model of the source. Hanks and McGuire (1981) presented a simple theoretical model that accurately predicts a_{max} for California earthquakes and corroborates the scaling of motions with magnitude that had been derived empirically (e.g., Joyner and Boore, 1981). The model treats ground motion as bandlimited finite-duration Gaussian white noise, with an amplitude spectrum given by Brune's (1970, 1971) model for shear radiation. Random-process theory is used to predict a_{max} from a_{rms} and the duration of strong shaking. The model was later extended to the prediction of peak velocity (v_{max}) and pseudo-relative-velocity spectra (*PSV*) by Boore (1983) and McGuire *et al.* (1984). Boore employed a stochastic time-domain simulation method and also used general equations from random-process theory. McGuire *et al.* obtained closed-form analytic solutions to the random-process theory equations through the use of suitable approximations.

Atkinson (1984) extended the method to prediction of a_{max} and v_{max} in ENA by using the Hanks and McGuire (1981) approach to obtain closed-form solutions. The relative enrichment of eastern earthquakes in high frequencies was taken into account through a suitably chosen high-frequency cut-off, and the attenuation of motions was modified to reflect the dominance of the *Lg* phase over *S* waves for distances greater than two crustal thicknesses. The model predictions for moderate earthquakes were verified by using eastern strong ground-motion data. Work performed simultaneously but independently by Boore, using the time-domain stochastic-simulation method, utilized similar assumptions and obtained similar results (Boore and Atkinson, 1984). In this paper, we extend the theoretical model used for ENA further, to the prediction of response spectra and relations between magnitude scales, using both time-domain simulation and random-process theory methods.

The main controversy over application of this method to the prediction of ground motion in ENA has concerned the choice of the underlying source model. In applications to the prediction of ground motion in western North America (WNA), Hanks and McGuire (1981), Boore (1983), and McGuire *et al.* (1984) all assume that the stress parameter controlling the strength of high-frequency radiation is a constant, with a value of 100 bars. This is in keeping with studies of moderate to large earthquakes around the world, which have shown that stress-drop values are nearly always between 1 and 200 bars and are apparently independent of source strength over 12 orders of magnitude in seismic moment (Kanamori and Anderson, 1975; Hanks, 1977; Boatwright, 1984). Atkinson (1984) adopted the constant stress-parameter assumption for the prediction of peak ground accelerations and velocities for ENA, and found good agreement between observations and predictions. In the context of the Brune source model (Brune, 1970, 1971), the constancy of the stress parameter is equivalent to the statement that seismic moment (M_0) times the corner frequency (f_0) raised to the third power is a constant [see equation (8)]. Nuttli

(1983a, b) has presented an alternate source-scaling model, for earthquakes in mid-plate regions, in which the stress-parameter increases with seismic moment such that $M_0 f_0^4$ would be constant in ENA. We refer to this as increasing-stress scaling. Nuttli (1983a, 1985) also finds that $M_0 f_0^3$ is constant for large plate-margin events. Such a fundamental difference in source spectra between mid-plate and plate-margin regions would have profound implications for earthquake engineering. For example, strong-motion data from many large WNA earthquakes could not adequately predict ENA motions, even if differences in regional attenuation were taken into account. Furthermore, for large earthquakes, the increase in stress-parameter with seismic moment implied by the increasing-stress model would cause very large ground motions if that model was used to extrapolate predictions that have been adjusted to match the ENA motions recorded from moderate earthquakes. Because the source-scaling issue is crucial to the prediction of ENA ground motion, this paper deals in some depth with the evidence for the two proposed scaling models. In our opinion, the weight of evidence supports the constant stress-parameter assumption, and our final results are therefore based on this model.

METHOD

Review of the basic method. We have used both the random-process theory and the time-domain method to predict ground motions. In both approaches, ground motion is modeled as bandlimited finite-duration white Gaussian noise in which the radiated energy is assumed to be distributed over a specified duration. The methods are quite general and can be used to predict many amplitude and instrument response parameters. The simple underlying physical model of the earthquake-source process requires surprisingly few parameters for its description.

The random-process approach to ground-motion prediction uses Parseval's theorem, which relates spectral amplitudes to root-mean-square (rms) amplitudes in the time domain. Equations from random-process theory (Cartwright and Longuet-Higgins, 1956) are then used to obtain expected values of peak amplitudes from the rms amplitudes. For details of the derivation, the reader is referred to Hanks and McGuire (1981), Boore (1983), McGuire *et al.* (1984), and Boore (1987). Application of the method to prediction of $a_{\max}$ and $v_{\max}$ in ENA is described in Atkinson (1984).

The time-domain simulation method (Boore, 1983) begins with the generation of a windowed-time series of bandlimited random white Gaussian noise with zero mean amplitude; the variance is chosen such that the spectral amplitude is unity on average. The spectrum of the windowed-time series is multiplied by the desired amplitude spectrum and transformed back to the time domain to yield a final time series. By repeating the process many times (changing just the seed of the pseudo-random number generator), a suite of representative time series is obtained. Depending on the form of the spectral amplitude, the time series can represent ground motions, such as velocity or acceleration, or instrument responses (and, of course, the derived accelerations can be used to find instrument responses in separate calculations). The instrument responses can be used to predict response spectra, or expected amplitudes and hence measured magnitudes on any seismographic instrument.

Both the time-domain and the random-process methods require specification of a basic spectral shape representing the radiation from the source. A number of other frequency-dependent functions are needed to specify the spectral energy at a given site; these include functions accounting for attenuation during propagation

and for instrument response (unless ground motions are being estimated). The spectra used in this paper are given by the following equations

$$R(f) = C \cdot S(f) \cdot D(f) \cdot I(f) \tag{1}$$

where C is a scaling factor, S is the source spectrum, D is the diminution function, and I specifies the type of motion being computed. Only $S(f)$ depends on seismic moment.

The scaling factor C is given by

$$C = \frac{\langle R_{\theta\phi} \rangle \cdot F \cdot V}{4\pi\rho\beta^3} \left(\frac{1}{r}\right), \tag{2}$$

where $\langle R_{\theta\phi} \rangle$ is the radiation pattern averaged over an appropriate range of azimuth and take-off angle (e.g., Boore and Boatwright, 1984), F accounts for free surface effects, V represents the partition of a vector into horizontal components [if needed, depending on the value of $\langle R_{\theta\phi} \rangle$ used], ρ and β are the density and shear velocity in the source region, and r is the hypocentral distance. Typically, the product $\langle R_{\theta\phi} \rangle \cdot F \cdot V$ has a value near unity, so some authors neglect these terms in their definition of source-spectral equations (e.g., Street and Turcotte, 1977).

The source function $S(f)$ is defined as

$$S(f) = M_0/[1 + (f/f_0)^2], \tag{3}$$

where M_0 is the seismic moment, and f_0 is the corner frequency. Joyner (1984) proposed a different source function; it is equivalent to equation (3) at high and low frequencies, but it has two corner frequencies. The two corners are related to one another by a constant factor (i.e., the spectra are self-similar) for earthquakes less than a certain size. Beyond a specified critical magnitude, however, one corner becomes fixed. The critical magnitude can be thought of as the magnitude at which the entire width of the fault plane has ruptured. Any further growth of the rupture surface occurs through lengthening of the fault. Joyner's source function is more general than the one in equation (3), but requires specification of several more parameters; there are no data with which to estimate these parameters for ENA. Fortunately, the two source functions lead to small differences in the predicted ground motions for earthquakes with magnitudes less than the critical magnitude, and the critical magnitude may be large enough that the earthquakes of most engineering concern will be smaller than the critical size earthquake.

The diminution function $D(f)$ models frequency-dependent functions that modify the spectral shape. These effects are represented by

$$D(f) = \exp[-\pi \cdot f \cdot r/Q(f) \cdot \beta] P(f, f_m), \tag{4}$$

where Q is the frequency-dependent quality factor, and P is a high-cut filter of arbitrary shape. Two forms of the P filter have been used in our previous work (e.g., Boore, 1986a)—the Butterworth filter

$$P(f) = [1 + (f/f_m)^8]^{-1/2}, \tag{5a}$$

and the exponential form advocated by Anderson and Hough (1984)

$$P(f) = \exp(-\pi\kappa f). \tag{5b}$$

The parameter κ in the exponential filter in equation (5b) can be related to f_m in several ways if it is desired to make the two high-cut filters approximately equivalent. For example, observations of spectra from some small to moderate earthquakes near Coalinga, California (J. Boatwright, oral communication, 1986), as well as the requirement that the exponential form be reduced to $1/e$ at $f = f_m$, leads to $\kappa = 1/\pi f_m$. On the other hand, for large earthquakes, the requirement that the rms acceleration be the same for both filters leads to $\kappa = 1/2\pi f_m$. In our application f_m is large enough (or the equivalent κ is small enough) that the choice of the high-cut filter makes little difference on the predicted ground motions in the frequency range of interest (generally, less than 10 Hz). In this paper, equation (5a) is used to represent the high-frequency filter.

Finally, the filter $I(f)$ is used to shape the spectrum so that the predicted motions correspond to the particular ground motion measure of interest. For example, if response spectra are to be computed, I is the response of an oscillator to ground displacement. If, on the other hand, ground velocity or ground acceleration are the quantities of interest, then

$$I(f) = (2\pi f)^p, \tag{6}$$

where $p = 1$ or 2 for velocity or acceleration, respectively.

The spectral shape implied by equation (1) features a constant long-period level which is (by definition) determined by the seismic moment of the event. Ignoring the effects of source finiteness, the amplitude spectrum for acceleration near the earthquake source increases as f^2 for frequencies below the source corner frequency f_0, then is constant for frequencies above f_0 until a cut-off frequency f_m is approached. The amplitude of the constant portion of the spectrum is proportional to $M_0 f_0^2$. Amplitudes decay rapidly for frequencies above f_m.

The source spectrum diminishes with distance from the source as a result of geometric spreading and anelastic attenuation. Geometric spreading reduces the entire spectrum, whereas anelastic attenuation and scattering combine to alter its shape by reducing high frequencies more rapidly with distance than lower frequencies [unless $Q(f)$ in equation (4) is proportional to frequency raised to a power of 1 or higher]. At large distances, the filtering can cause the "flat" portion of the spectrum to slope significantly, thereby obscuring the corner frequency.

The source spectrum included in equation (1) represents the generation of shear (S) waves. It is well known that in ENA, Lg waves carry most of the energy at large distances from the source. [Lg waves are multi-mode guided surface waves consisting of a complex interference of multiply-reflected S waves (Kennett, 1985).] Inherent in using equation (1) for Lg waves is the assumption that the transfer function due to wave propagation is not dependent on frequency. Support for this assumption comes from the modeling studies of Herrmann and Kijko (1983) and Campillo *et al.* (1985).

The distance beyond which the dominant ground-motion signal can be better described by the Lg phase, rather than by S body waves, is approximately that of

two crustal thicknesses (Herrmann and Kijko, 1983), or roughly 100 km. The transition from body-wave to surface-wave content is modeled in our predictions by a change in the geometric spreading factor at a cross-over distance of r_x from $1/r$ to $1/(rr_x)^{1/2}$ in equation (2) (the factor of r_x guarantees continuity of the motions at $r = r_x$). Although a number of the results presented later were computed with $r_x = 100$ km, an effort was made to smooth out the kink at $r = r_x$ for the calculations on which the prediction equations are based. To produce the smoothing, we averaged the results from 30 simulations in which r_x was chosen randomly between 60 and 170 km, assuming a uniform distribution for r_x between these limits.

An additional modification for large distances is made to account for the increase in duration of motion with distance. In modeling the ground motion near the source, it is assumed that the duration associated with generation of the peak motion or response is the faulting duration, estimated as $1/f_0$ (Hanks and McGuire, 1981). This will be referred to here as the source duration (T_s). Following Herrmann (1985), the duration at any distance r is approximately $T_s + 0.05r$. Herrmann (1985) has found that the increase of duration with distance, combined with the geometric spreading factor of $1/r^{1/2}$ for surface waves, results in an overall geometric attenuation close to the factor of $1/r^{5/6}$ that is usually associated with *Lg* waves (e.g., Nuttli, 1979).

A further refinement to the basic random-process theory is required when making estimates of response spectra. The random-process theory approach assumes a stationary time series, but for small to moderate magnitude earthquakes and low-frequency, lightly damped oscillators, the duration of motion is too short to generate a pseudo-stationary response. We have employed modifications to the duration definition, proposed by Boore and Joyner (1984), that allow random-process theory to be used in the computation of the response of such oscillators. To check the accuracy of this approach, peak motions for the model parameters considered in this paper were computed with random-process theory and with time-domain simulations; the peak motions were usually within 0.05 log units of one another. For computational convenience, we have used the random-process theory results for all motions reported in this paper, unless noted otherwise.

Two modifications to the basic method described in Boore (1983) have been made in subsequent studies (Atkinson, 1984; Boore, 1986a) but are not included here. Atkinson (1984) used arguments advanced by Joyner and Boore (1981) to limit near-source ground motions from large magnitude events. These reductions attempted to model the effect of finite source dimensions; as the distance to the source becomes small compared to the dimensions of the source, then only a portion of the source may be effective in exciting ground motion. For magnitude 7 events, this effect is predicted to reduce amplitudes by 30 to 50 per cent at a distance of 10 km, with the discrepancy diminishing gradually to zero near 50 km. For smaller magnitudes, the effect is not as great; for magnitude 6 (or smaller) events at 10 km, the difference would be less than 20 per cent. Because these modifications are significant only over a limited magnitude and distance range and must be considered hypothetical due to lack of ENA data for events in this range, they are neglected in these predictions. This implies that our results may overpredict ground motions from magnitude 7 events at distances less than approximately 30 km.

Another modification which is not considered here is a broadband site amplification factor to account for the fact that because of weathering and related effects, near-surface rock may have lower seismic impedance than rock at seismogenic depths. This difference in seismic impedance can lead to amplification of the surface

motions by as much as a factor of 2.0 for California crustal conditions (Boore, 1986a, 1987). In contrast, typical ENA crustal profiles (Yang and Aggarwal, 1981) indicate that the amplification in ENA would be less than a factor of 1.2. This is not considered significant in view of other uncertainties and is therefore neglected in this paper. The effect can be easily included for any known (i.e., site-specific) crustal profile, however, by multiplying the hard-bedrock results presented here by the square root of the effective ratio of seismic impedance (see Boore, 1986a, 1987).

Required input parameters. Application of the stochastic model to prediction of ground motion or response measures in ENA requires estimation of the various factors in the numerator of the factor C [equation (2)], the regional crustal material properties ρ and β, and the regional quality factor Q. A source-scaling function, describing how spectral amplitude levels and corners are related to seismic moment, is also required; since this is the most contentious input, it will be discussed in detail in the next section.

The constants in factor C are taken as follows: $\langle R_{\theta\phi} \rangle = 0.55$ (Boore and Boatwright, 1984), $F = 2.0$, and $V = 0.71$. For average crustal properties, we use $\rho = 2.7$ gm/cm^3 and $\beta = 3.5$ km/sec; these values are appropriate for the seismogenic depths in ENA, which we assume are centered near 10 km. The shear velocity β was determined from the compressional velocity found at that depth in interpretations of seismic profiling in both Maine and the Mississippi embayment (W. Mooney and M. Andrews, oral communication, 1985); a Poisson's ratio of 0.25 was assumed.

Several Q models based on regional seismographic data have been derived for ENA. The range of proposed models is illustrated by comparing the recent results of Dwyer *et al.* (1984), Hasegawa (1985), and Shin and Herrmann (1987). Shin and Herrmann (1987) studied *Lg* propagation characteristics through spectral analysis of New Brunswick earthquakes digitally recorded by the Eastern Canada Telemetered Network (ECTN) and obtained the relation

$$Q = 500 f^{0.65}. \tag{7a}$$

Hasegawa (1985) analyzed ECTN recordings of *Lg* waves from a large number of ENA shield earthquakes, which excluded the New Brunswick earthquakes, and obtained

$$Q = 900 f^{0.2}. \tag{7b}$$

For the Central United States (which we include in this paper as part of ENA), Dwyer *et al.* (1984) performed similar analyses based on recordings of the central Mississippi Valley seismic network and obtained

$$Q = 210 f^{0.78} \tag{7c}$$

for *Lg* wave attenuation. The differences between these Q models could be due to either regional variations in crustal structure or differences in methodology. The Q values obtained from equation (7a) lead to response values intermediate to those obtained using equations (7b) and (7c), and they are adopted in this study as a reasonable compromise.

The cut-off frequency f_m has been interpreted as being alternatively a source or a site parameter (Hanks, 1982; Papageorgiou and Aki, 1983). According to equation (5a), its effects can be represented by a single-valued cut-off frequency. Typical

values are 15 Hz for rock sites in the Western United States (Hanks, 1982) and 50 Hz for ENA hard-rock sites (Atkinson, 1984); the latter value, based on limited data from New Brunswick and Ontario earthquakes, will be used in this paper. The higher f_m value for ENA reflects the harder, more competent rocks generally found in ENA, as compared to the Western United States. Considerably lower values could occur on soil sites; therefore, the ground motion and spectral response predictions in our paper are restricted to sites underlain by competent rock.

Source-Scaling Models

The manner in which source spectra are scaled with magnitude (or seismic moment) is an important input assumption to these analyses. This scaling is controlled by the two remaining unspecified parameters in our model: seismic moment, M_0, and corner frequency, f_0. On physical grounds, and for simplicity of application, it is natural to seek a relation between these parameters. Such a relation would reduce the scaling of peak motions to a function of seismic moment only. We consider two relations between M_0 and f_0: the first due to Brune (1970, 1971) (constant-stress), and the second due to Nuttli (1983b) (increasing-stress). Other relations are possible, involving seismic moment and several low- and high-frequency spectral corners (e.g., Joyner, 1984; Irikura and Aki, 1985; Faccioli, 1986), but we have chosen to use the simplest relations.

The relation between M_0 and f_0 for the constant-stress model can be expressed as follows:

$$f_0 = 4.9 \times 10^6 \beta (\Delta\sigma / M_0)^{1/3}, \tag{8}$$

with β in km/sec, $\Delta\sigma$ in bars, and M_0 in dyne-cm. In Brune's derivation, $\Delta\sigma$ is the static stress drop. Because the amplitude of the spectrum above the corner frequency f_0 is proportional to the square of f_0, the parameter $\Delta\sigma$ exerts a strong influence on the high-frequency radiation. The stress controlling this radiation is known by several names; we prefer to refer to it simply as the stress parameter and thereby not attach any physical significance in terms of faulting models. The simplification in the scaling of the source spectra is obtained by making the assumption that the stress parameter is constant. In that case, corner frequency is proportional to the inverse cube root of the moment; in other words, $M_0 f_0^3$ is a constant.

The constant-stress model was based primarily on analyses of $M_0 - f_0$ data from plate-margin earthquakes. By contrast, the increasing-stress model was based on a set of scaling relations that would agree with observations between different magnitude scales in mid-plate regions (Nuttli, 1983a). These scaling relations led to the conclusion that $M_0 f_0^4$ is constant, implying a stress-parameter that increases with seismic moment. This relation was consistent with the $M_0 - f_0$ values derived for ENA earthquakes by Street *et al.* (1975). Nuttli (1983a) therefore concluded that a fundamental difference exists between mid-plate and plate-margin events. This conclusion is extremely important because it implies that data from a plate-margin region such as WNA cannot be used to aid in predicting ground motions in mid-plate regions such as ENA; this implication would invalidate almost all empirical ENA ground-motion relations derived to date [one exception being the semi-theoretical Herrmann and Nuttli (1984) relation, which uses existing data (near magnitude 5) to set the absolute level of curves whose magnitude scaling is predicted by the assumption that $M_0 f_0^4$ is a constant]. Because the scaling relation between

M_0 and f_0 plays a fundamental role in our calculations, it is clearly important to investigate in some detail the relative merits of the two scaling relations.

The theoretical model can be used to compare how well the two relations can predict the modest amount of ENA strong ground motion. Atkinson (1984) found good agreement between the stochastic-model predictions and the observed $a_{\max}$ and $v_{\max}$ values, using $\Delta\sigma = 100$ bars. From equation (8), with $\beta = 3.5$ km/sec, this implies that

$$f_0 = 7.96 \times 10^7 M_0^{-1/3}, \tag{9a}$$

where the units of f_0 and M_0 are Hz and dyne-cm, respectively. By contrast, the increasing-stress relation proposed by Nuttli [1983b, equation (7)] is given by

$$f_0 = 3.55 \times 10^5 M_0^{-1/4}. \tag{9b}$$

The moment dependence of the stress-parameter, corresponding to equation (9b), can be obtained by eliminating f_0 from equations (8) and (9b).

Equations (9a) and (9b) predict the same corner frequency, and thus the same ground motions, when $M_0 = 1.6 \times 10^{28}$ dyne-cm; this corresponds to a moment magnitude of $\boldsymbol{M} = 8.1$, using the moment-magnitude definition of Hanks and Kanamori (1979)

$$\boldsymbol{M} = \tfrac{2}{3} \log M_0 - 10.7. \tag{10}$$

For magnitudes less than 8.1, the increasing stress-parameter scaling predicts lower corner frequencies, and thus smaller ground motions, than does the constant stress-parameter scaling when the predictions are made using our theoretical method. By contrast, if the increasing stress-parameter scaling is used as a guide for extrapolating estimates from the small-magnitude earthquake data to larger earthquakes, without regard to theoretically predicted absolute values, the stronger seismic-moment dependence will lead to larger estimates of motions, as compared to those predicted by the constant-stress scaling.

These points are illustrated in Figure 1, which shows predicted pseudo-response velocity (PSV) for two frequencies at two distances; brackets indicate the spread of the data (estimated from Figure 8 in this paper). The figure shows the stronger dependence on magnitude of motion from increasing-stress scaling and the convergence of predictions from both scaling relations at $\boldsymbol{M} = 8.1$. It also indicates that the PSV predicted from the increasing-stress scaling does not agree with the data. No free parameters, such as stress drop, are available to improve this fit. We conclude that the increasing-stress scaling is inconsistent with ENA ground motion observations. On the other hand, note that the good fit of the predictions from the constant-stress scaling do not in themselves indicate the validity of this scaling; a stricter test of the scaling would be its ability to predict the slope of the PSV versus magnitude. Current data do not allow such a test.

There are further reasons to question the use of the increasing-stress scaling for predictions of strong ground motions. In our opinion, the data that led Nuttli to suggest that the scaling of mid-plate and plate-margin earthquakes is fundamentally different are inconclusive. We have plotted data from both mid-plate and plate-margin earthquakes on the same graph to allow visual comparisons (Figure 2), using

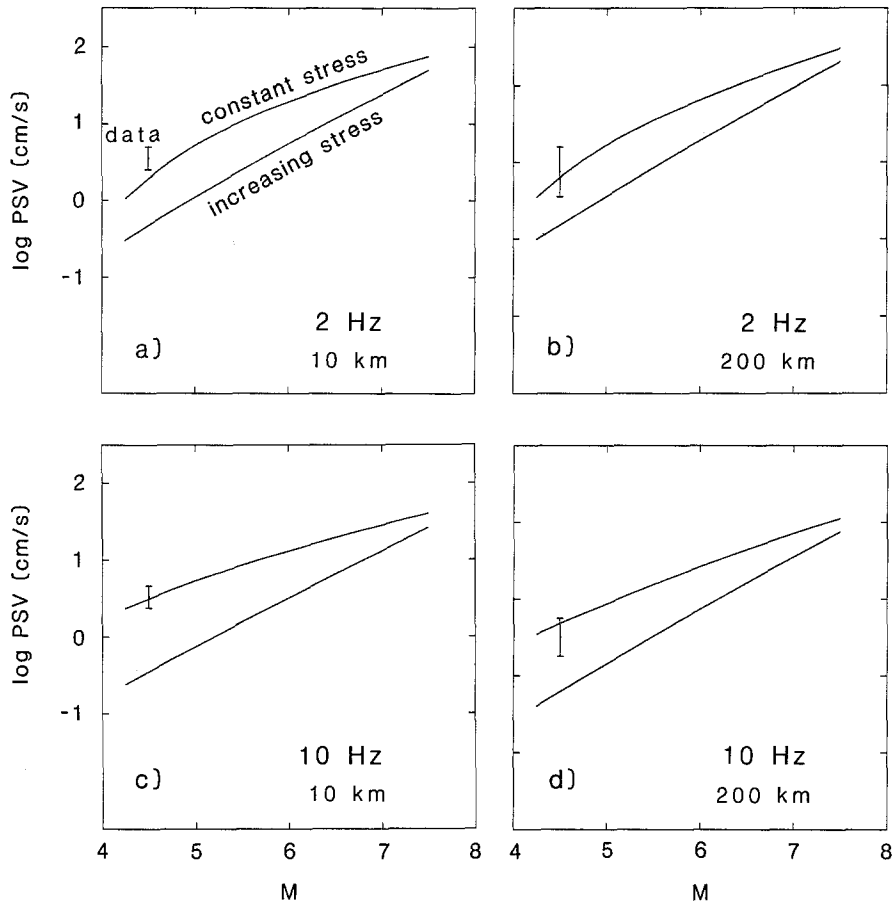

FIG. 1. Predicted dependence of 5 per cent damped pseudo-velocity response spectra (*PSV*) on moment magnitude (***M***) for oscillator frequencies of 2 and 10 Hz and distances of 10 and 200 km. The theoretical predictions are given by the curves; the one labeled *constant stress* used equation (9a), and the one labeled *increasing stress* used equation (9b) to relate seismic moment to corner frequency. The data are represented by the brackets and were estimated from Figure 7.

essentially the same data used by Nuttli (1983a, b). For several reasons, we have separated the mid-plate data set into two groups: pre- and post-1963. The year 1963 was chosen because that was when installation of the World-Wide Standardized Seismograph Network began. Before that time, magnitude values for the earthquakes in the mid-plate data set were generally determined from multi-mode guided surface waves at regional distances (m_{Lg}). The magnitudes from the more recent earthquakes are largely from teleseismic body waves (m_b). Also, the pre-1963 data are almost entirely from ENA, whereas many of the post-1963 data are from mid-plate regions in other parts of the world.

There is a clear difference between pre- and post-1963 $m_b - \boldsymbol{M}$ relations within mid-plate data, as noted by Atkinson (1984). One possible reason for this separation is that the magnitudes are fundamentally different; the equivalence of teleseismic m_b and m_{Lg} determined from data at regional distances has not been demonstrated for earthquakes with magnitude larger than 5. The lines in Figure 2 show the mean $m_b - \boldsymbol{M}$ relations suggested by Nuttli (1983a, written communication, 1984) for mid-plate and plate-margin earthquakes. To some extent the mid-plate line lies above the plate-margin line because it reflects an average of the pre- and post-1963

data. If these data are fundamentally different, this could bias the conclusion regarding differences between earthquakes in mid-plate and plate-margin regions.

Concentrating now on the post-1963 data, at first glance there seems to be little difference in m_b versus $\boldsymbol{M}$ data between mid-plate and plate-margin regions. More careful inspection, however, reveals that for a given $\boldsymbol{M}$, the mean value of m_b may be somewhat lower for plate-margin earthquakes than for mid-plate earthquakes. Regional variations in $m_b - \boldsymbol{M}$ relations have been demonstrated by several authors (Kanamori and Anderson, 1975; Liu and Kanamori, 1980). There are a number of possible reasons for such regional differences. For example, the plate-margin data set may be enriched in strike-slip earthquakes relative to the mid-plate data set; the *P*-wave radiation pattern for teleseismic recordings of strike-slip events can lead to anomalously low m_b values for these events, thus producing a bias in the m_b values for plate-margin earthquakes. Another explanation could be a difference in the value of the stress-parameter (as opposed to differences in its scaling with moment). In order to support a difference in the nature of scaling relations, as suggested by Nuttli (1983a), there would need to be a difference in the *slope* of $m_b - \boldsymbol{M}$ between the two types of data. The scatter in the data and the limited moment range of mid-plate earthquakes make it difficult to differentiate between a constant-stress scaling and an increasing-stress scaling. The data in Figure 2 are not a compelling reason for concluding that a fundamental difference exists between mid-plate and plate-margin events.

Further support for the constant-stress scaling comes from Somerville *et al.* (1987), who use moments and source durations based on analysis of teleseismic recordings of ENA earthquakes to argue against the $M_0 f_0^4$ constant postulate. They find that, for moderate to large earthquakes, the stress parameter is about 100 bars.

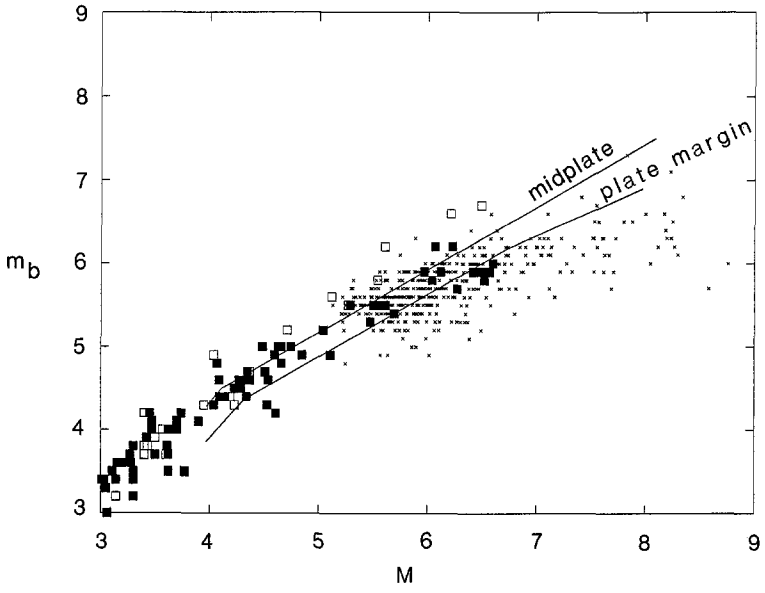

FIG. 2. Body-wave (m_b) versus moment ($\boldsymbol{M}$) magnitudes for mid-plate earthquakes (squares) and plate-margin earthquakes (X's). The mid-plate earthquakes [from a compilation by Nuttli (1983a)] have been separated into those occurring before and after 1963 (empty and filled squares, respectively). The pre-1963 m_b values may actually represent m_{Lg} in most cases. The lines show Nuttli's (1983a; written communication, 1984) m_b versus $\boldsymbol{M}$ relations. Because they are based on the first few cycles of the *P*-wave train, the m_b values for the earthquakes with moment magnitudes greater than about 7.0 are underestimates of the actual short-period energy radiation (Houston and Kanamori, 1986; Boore, 1986a).

Chael (1987) has studied spectral ratios of the 1982 Miramichi, New Brunswick, main shock and 11 of its aftershocks recorded at the same station. This set of events had m_{Lg} values between 3.3 and 5.8. He found that the ratios strongly supported the source model given in equation (3). In agreement with many source studies (e.g., those cited in Boore, 1986b), increasing-stress scaling, and thus a breakdown in similarity, was indicated for the smaller events. For the larger events ($m_{Lg} > 5$) of interest to this study, Chael's data cannot distinguish between the constant-stress scaling and increasing-stress scaling.

Finally, Haar *et al.* (1986) found that, for the few ENA earthquakes having both close-in and more distant recordings, the corner frequencies estimated from the close-in recordings are roughly in agreement with those predicted for a 100-bar stress-parameter. For these same events, the corner frequencies estimated from *Lg* waves, using the method of Street *et al.* (1975), are significantly smaller, in the same sense as predicted by equations (9), than those determined from close-in recordings. This result is not surprising because observed corner frequencies decrease with distance due to the effects of anelastic attenuation, as noted by Hasegawa (1983). Finn *et al.* (1986) show that correcting *Lg* spectra for attenuation [this was not done in the Street *et al.* (1975) study] leads to significant reductions in the difference between corner frequencies estimated from the close-in and more distant recordings.

In summary, the evidence favoring an increasing-stress scaling is inconclusive. Constant-stress scaling (for magnitudes greater than 5) appears to be supported by the limited ENA data currently available, and has been successful in predicting WNA ground motions. We have therefore adopted the constant-stress scaling in predicted ground motions in ENA. We acknowledge, however, that there are too few data from large earthquakes in ENA to prove that this scaling is correct over the entire magnitude range.

A value must be set for the stress-parameter. We have chosen $\Delta\sigma = 100$ bars in view of the results of Somerville *et al.* (1987), Haar *et al.* (1986), and because using it in the stochastic model leads to predictions of $a_{\max}$ and $v_{\max}$ (Atkinson, 1984), as well as *PSV* (Figure 1), in agreement with the data. One hundred bars is considered to be a reasonable first approximation to $\Delta\sigma$, and it may be refined as more data for large ENA earthquakes are obtained.

Boore (1986a) found that data from WNA (primarily from California) at rock sites could be predicted with a stress-parameter of 50 bars, if amplification of the waves due to the decreasing rigidity of the near-surface rock was taken into account. This amplification, which is dependent on the impedance ratio between rocks within a quarter wavelength of the surface and those near the earthquake hypocenter, was estimated to be about a factor of 2 at frequencies of several Hertz. We do not expect as much amplification at rock sites in ENA, for the rock is generally much more competent than in the WNA rock sites from which strong motion data have been obtained. Based on several velocity profiles (Yang and Aggarwal, 1981; E. Cranswick, oral communication, 1985), we estimate amplifications of only 1.05 to 1.2. These are so small in comparison with the other uncertainties that we have neglected bedrock site amplification. If we are correct in the relative amplification of typical ENA and WNA rock sites, the conclusion from fitting the models to data is that the average stress parameters are also different.

Choice of Magnitude as Explanatory Variable

The predictive relations for ground-motion parameters can be formulated in terms of any magnitude scale. For predicting ground motions from a physical model

of the source, moment magnitude $\boldsymbol{M}$ is the most logical choice, as it is the magnitude most closely related to physical characteristics of the source. There is, furthermore, some hope of using independent information, such as geologic slip rates, to make rational estimates of $\boldsymbol{M}$ for future earthquakes. Other magnitude scales are actually instrument-filtered ground-motion measures, and therefore the specification of the magnitude of a future earthquake is equivalent in some sense to specifying ground motion directly. In our paper, the predicted ground-motion estimates are given in terms of $\boldsymbol{M}$. In practice, however, ground motions are usually desired for earthquakes whose sizes are given in terms of m_{Lg}, since this is the magnitude scale upon which current earthquake catalogs are based; $\boldsymbol{M}$ is not routinely determined for eastern events. Bowing to convention, we provide in this section a discussion of m_{Lg} and suggest a relation to convert m_{Lg} to $\boldsymbol{M}$.

In order to make a valid comparison between measured and predicted m_{Lg}, it is essential to ensure consistency of the definition of magnitude. For this reason, we reevaluated the available ENA data to obtain a subset of $m_{Lg} - \boldsymbol{M}$ data that would conform to Nuttli's (1973) original definition of m_{Lg}. This is

$$m_{Lg} = \begin{cases} 3.75 + 0.90 \log(r/111) + \log(A/T), & 56 \leqq r \leqq 445; \\ 3.30 + 1.66 \log(r/111) + \log(A/T), & 445 \leqq r \leqq 3336, \end{cases} \tag{11}$$

where r = distance in kilometers, A = peak vertical ground motion in micrometers, and T = period of the peak motion in seconds. The emphasis of our study is on the larger events ($m_{Lg} \geqq 4.5$), the most important of which are five historic earthquakes of $m_{Lg} > 5$ studied by Street and Turcotte (1977). Using the station data provided in their paper, we recomputed m_{Lg} for these events. Our values of m_{Lg} differ from those of Street and Turcotte for two reasons: most importantly, we use all station data to determine A/T, whereas Street and Turcotte calculated m_{Lg} only if the predominant period was near 1 sec. Furthermore, we assumed that a ratio of horizontal to vertical motion (H/V) is 1.4; Street and Turcotte (1977) used a factor of 3. Our factor follows from relations between mean and largest single horizontal component (Joyner and Boore, 1982), largest single component and horizontal vector motion (Mostaghel and Ahmade, 1982), and horizontal vector motion and vertical motion (Street, 1978; Gupta *et al.*, 1982). Our analysis indicates that, for the broadband intermediate-period instruments considered, Nuttli's (1973) m_{Lg} scale does a very good job for these historic earthquakes; the magnitude residuals (not shown) indicated little dependence on predominant period, instrument type, and distance, for magnitudes $m_{Lg} > 5$ with $T \leqq 10$ sec. The m_{Lg} values we obtained are generally within 0.2 units of those of Street and Turcotte (1977); the major exception is the 1925 La Malbaie, Quebec, earthquake, for which they obtained m_{Lg} = 6.6 (based on only one station), using the 1-sec magnitude definition, and we obtained m_{Lg} = 7.0 (using the average from nine stations).

For consistency, we also adjusted Street and Turcotte's moment magnitude estimates according to the constant factors (radiation pattern and free surface) of our source spectrum definition [equation (2)], crustal properties, and assumed H/V ratio. This adjustment generally resulted in an increase in moment by a factor of about 2 (equivalent to 0.2 moment magnitude units).

Table 1 and Figure 3 present the $m_{Lg} - \boldsymbol{M}$ data set, which consists of the five earthquakes discussed above, plus eight recent earthquakes of $m_{Lg} \geqq 4.5$ for which we could obtain reliable estimates of m_{Lg} (by the Nuttli 1973 definition) and $\boldsymbol{M}$. To give an indication of the possible range of magnitude values, we present our values and those from a variety of sources. To our knowledge, Figure 3 is the only such

TABLE 1

MULTI-MODE GUIDED SURFACE-WAVE (m_{Lg}) AND MOMENT (M) MAGNITUDES FOR ENA EARTHQUAKES

Date	m^*_{Lg}	M^*
3 01 25	7.0 (b), 6.6 (a)	6.5 (b), 7.0 (d), 6.8 (e), 6.2 (a)
8 12 29	5.4 (b), 5.2 (a)	4.9 (b), 4.7 (a)
11 01 35	6.3 (b), 6.2 (a)	5.8 (b), 6.4 (d), 6.4 (e), 5.6 (a)
12 20 40	5.7 (b), 5.5 (a)	5.5 (b), 5.5 (e), 5.3 (a)
9 05 44	5.9 (b), 5.8 (a)	5.8 (b), 5.8 (e), 5.6 (a)
8 19 79	5.0 (i)	4.8 (i)
1 09 82	5.7 (c)	5.5 (o), 5.6 (p), 5.5 (q), 5.4 (r), 5.4 (s)
1 11 82	5.5 (c), 5.5 (m)	5.2 (n), 5.2 (g), 5.3 (h), 4.8 (j)
1 19 82	4.8 (c)	4.4 (n), 4.3 (g), 4.5 (h)
3 31 82	4.8 (c)	4.0 (h), 4.2 (j), 4.4 (f)
6 16 82	4.6 (c)	4.0 (f), 3.8 (j)
10 07 83	5.6 (c), 5.3 (m)	5.0 (n), 4.9 (k), 5.1 (l)
1 31 86	5.3 (c)	4.8 (n), 4.6 (t), 5.0 (u)

* First value listed is our preferred value. a = Street and Turcotte (1977); b = our revised magnitudes (see text), based on data in Street and Turcotte (1977); c = Geophysics Division, Geological Survey of Canada, Ottawa, Canada; d = from body waves, Ebel *et al.* (1986); e = from surface waves, Ebel *et al.* (1986); f = from ECTN spectra (D. Boore, unpublished data); g = Nguyen and Herrmann (1984); h = J. Boatwright (written communication, 1984); i = Hasegawa (1983); j = Street (1984); k = G. Suarez (written communication to J. Boatwright, 1984); l = Wu (1984); m = Seismological Notes, *Bull. Seism. Soc. Am.*, vol. 74, p. 1505; n = average of next two values; o = average of next four values; p = Choy *et al.* (1983), corrected for neglected factor of 1.8 to account for free surface effect (J. Boatwright, oral communication, 1986); q = Wetmiller *et al.* (1984); r = Nábělek (1984); s = Somerville *et al.* (1987); t = R. Herrmann (oral communication, 1986); u = A. Dziewonski (oral presentation, American Geophysical Union Spring Meeting, 1986).

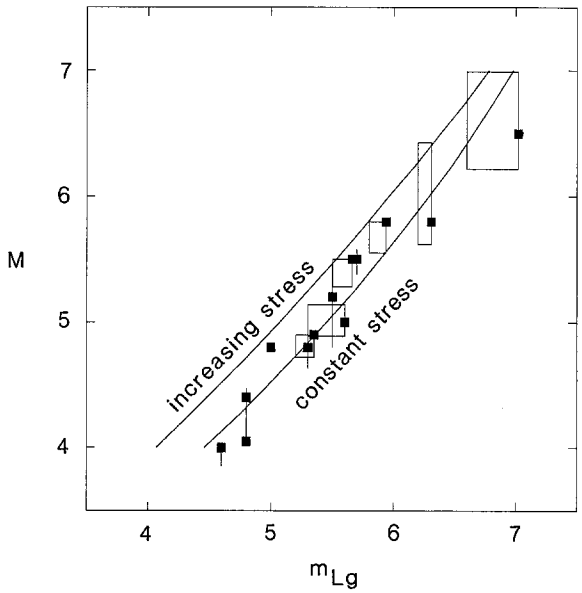

FIG. 3. Predicted relations between guided surface-wave (m_{Lg}) and moment (M) magnitudes for two scaling relations (constant and increasing stress). M is the ordinate in this figure (rather than the abscissa as in Figure 2) because in applications it is necessary to find M given m_{Lg}. Data are the ENA subset of Table 1. Squares show preferred values, and boxes (and lines) enclose other published estimates. The theoretical results are for a Wood-Anderson instrument, which was fairly commonly used in deriving the observed values of m_{Lg}; the theoretical values of m_{Lg} are in the middle of those predicted for other instruments used to determine magnitudes of ENA earthquakes (Table 2).

plot in print that shows an ENA data set (for larger earthquakes) for which all $m_{Lg} - \boldsymbol{M}$ values have been determined according to a consistent definition. We therefore believe these data are more reliable, and certainly less ambiguous, than the larger data set of Figure 2, which contains a mixture of magnitude definitions of uncertain equivalence.

Random-process theory was used to estimate the characteristic period and peak amplitude as recorded on several standard instruments, and these values were converted into m_{Lg} by using the definition of equation (11). The predicted motions were reduced by a factor of 0.7 to convert from mean horizontal to vertical motion. Table 2 lists predicted m_{Lg} for earthquakes of two sizes as recorded on a variety of instruments at a distance of 800 km (roughly, the median distance in m_{Lg} magnitude measurements for data of Street and Turcotte). As suggested empirically, the magnitude determination is relatively insensitive to type of instrument.

The predicted magnitudes are shown in Figure 3 for both the increasing-stress models and constant-stress models [as specified in equations (9)]. The agreement of the constant-stress model with the magnitude data is excellent, whereas that for the increasing-stress model appears rather poor. This does not prove that the constant-stress model is correct, because by changing the assumed $Q(f)$ function for the prediction, it is possible to make the increasing-stress model appear to be a better fit. Rather, the plot is intended to show that the model we have used in our predictions of response spectral and ground-motion parameters is consistent with the $m_{Lg} - \boldsymbol{M}$ data. The plot also provides some validation for our predictions of the motions from the larger earthquakes for which no close-in data are available, albeit the check is at a distance of no concern for engineering design.

Using least-squares linear regression, we fit a curve to the predicted magnitudes from the constant-stress model, arriving at the following equation valid for $4 \leqq m_{Lg} \leqq 7$

$$\boldsymbol{M} = 2.715 - 0.277 m_{Lg} + 0.127 m_{Lg}^2. \tag{12}$$

We have given $\boldsymbol{M}$ as a function of m_{Lg}, rather than vice-versa, as a convenience in application.

Ground-Motion Predictions

Results. The predictions of ground motions for the standard model are provided in both graphic and equation form. All curves refer to predicted hard-bedrock motions. There may be significant frequency-dependent amplification by local site conditions that should be addressed on a site-specific basis. Soil amplifications can be very significant, amplifying motions by as much as a factor of 10 or more. In

TABLE 2

Predictions of Multi-Mode Guided Surface-Wave Magnitudes (m_{Lg}), on Five Instruments 800 km from $M = 4.5$ and $M = 6.5$ Earthquakes

Instrument	$M = 4.5$	$M = 6.5$
Bosch	4.96	6.68
ECTN	4.98	6.43
Milne-Shaw	4.98	6.84
Wood-Anderson	4.98	6.65
WWSSN SP	4.86	6.47

addition, some areas characterized by soft or weathered near-surface rocks may show amplifications of as much as a factor of 2 with respect to hard-rock sites.

The distance attenuation of PSV and a_{max} are given in Figure 4, and the magnitude and the frequency dependence of PSV at fixed distance are shown in Figures 5 and 6, respectively. As seen in Figure 4, the scaling of ground motion with magnitude is nonlinear, especially for lower frequency oscillators. Furthermore, the shape of the attenuation curves can be magnitude-dependent. We wish to express the predictions in equation form, and these features demand a somewhat complicated functional form to adequately reproduce the calculated points. The data for a fixed magnitude were fit to equation (13a), which represents the theoretical form of decay due to geometric and anelastic attenuation. The data consisted of theoretical predictions at 11 distances, distributed at equal logarithmic intervals between 10 and 100 km, and 11 magnitudes, at equal intervals between 5.0 and 7.5. Only distances from 10 to 100 km were considered, thus avoiding the necessity to fit the bump formed by the transition to a geometrical attenuation of $1/r^{1/2}$ near 100 km. (Except in unusual circumstances, most damaging motions will probably be produced by earthquakes within 100 km.) The resulting distance coefficients were fit to a polynomial in $\boldsymbol{M}$. It was necessary to use a polynomial for the magnitude dependence, rather than a

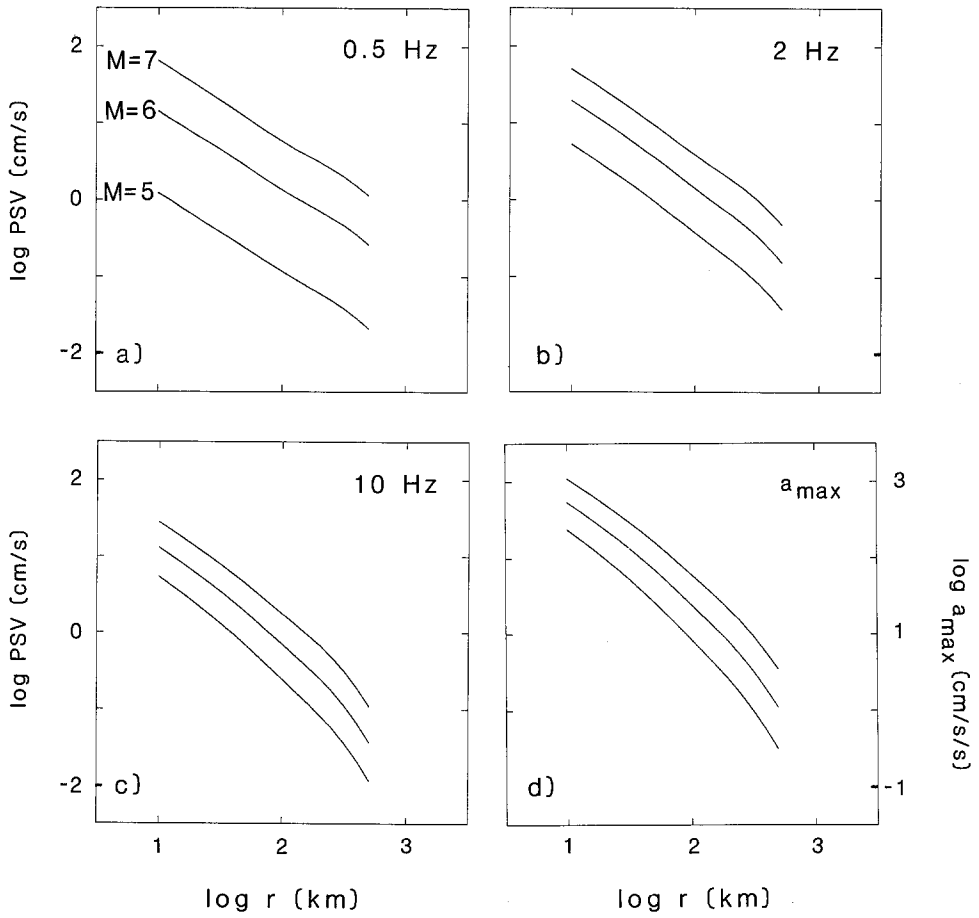

FIG. 4. Predictions of distance (r) dependence of 5 per cent damped pseudo-velocity response spectra (PSV), at three oscillator frequencies, and peak acceleration for moment magnitudes of 5, 6, and 7. Each curve is an average of 30 runs, using randomly chosen cross-over distances r_x (see text).

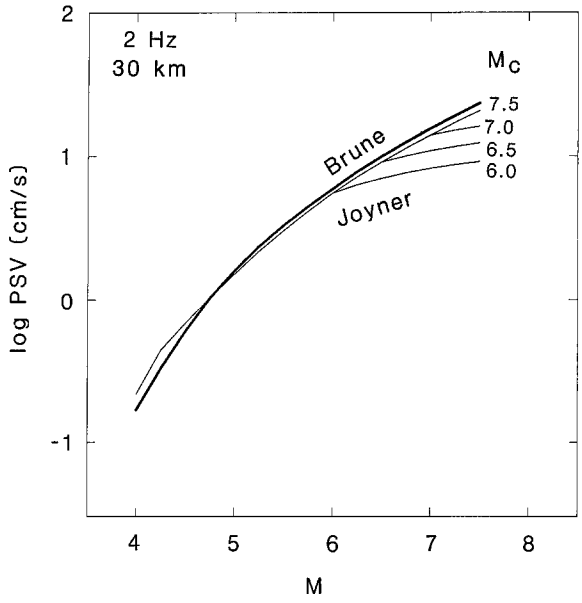

FIG. 5. Magnitude scaling of 2 Hz, 5 per cent damped pseudo-velocity response spectra (*PSV*) at 30 km distance, for Brune and Joyner source-scaling models. Both models assume a stress parameter of 100 bars, with $r_x = 100$ km, and the results for the Joyner model are shown for critical magnitudes (beyond which the source is no longer self-similar) of 6.0, 6.5, 7.0, and 7.5.

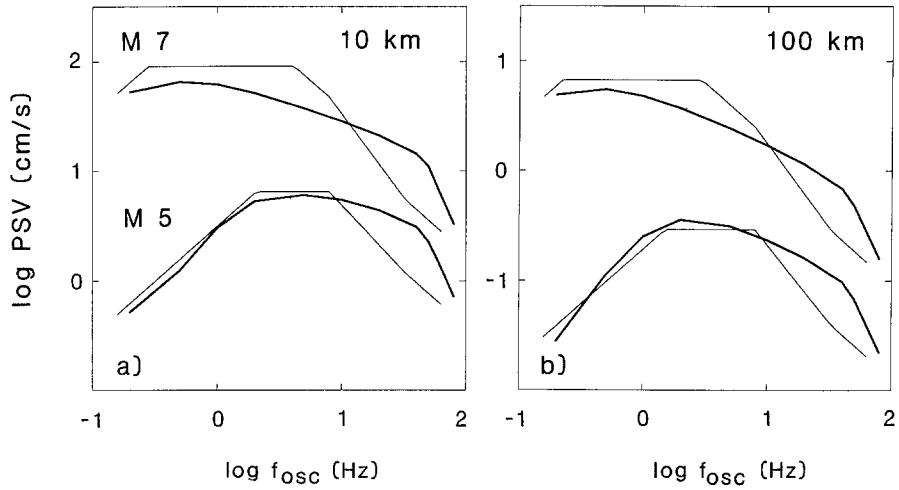

FIG. 6. Predicted 5 per cent damped pseudo-velocity response spectra (*PSV*) at 10 and 100 km as a function of oscillator frequency (f_{osc}). Predictions from the model in this paper are given by the heavy curves, with $r_x = 100$ km. The solid lines were obtained from the peak velocity and acceleration predicted from the model by applying median amplification factors from Newmark and Hall (1982; Table 1), with faring to the high-frequency asymptote beginning at 8 Hz and ending at 33 Hz (see Figure 5 in Newmark and Hall, 1982).

theoretical form based on source-spectral scaling, because of nonlinear effects caused by nonstationarity of the response of oscillators to smaller magnitude earthquakes. These effects are particularly pronounced for low-frequency oscillators. The predictions are calculated by the equations

$$\log y = c_0 + c_1 r - \log r \tag{13a}$$

and

$$c_i = \xi_0{}^i + \xi_1{}^i(\boldsymbol{M} - 6) + \xi_2{}^i(\boldsymbol{M} - 6)^2 + \xi_3{}^i(\boldsymbol{M} - 6)^3, \quad i = 0, 1 \qquad (13b)$$

where y is a ground-motion parameter. The coefficients ξ are given in Table 3. To reduce the number of coefficients needed, only enough are included so that the overall standard deviation of the fit is less than 0.02 log units. Even so, the curves are a better fit to the calculated points for large earthquakes than for smaller events. In no case, however, is the misfit as large as 0.08 log units. These uncertainties refer only to the ability of the function form to fit the calculations. They do not include natural scatter due to physical variability in source parameters, propagation characteristics, or site conditions. This natural scatter is much larger than that due to the functional form. Previous studies based on California data indicate that the overall scatter of observed ground motions about the values predicted by regional ground-motion relations is in the range of $\sigma_{\log y} = 0.16$ (Campbell, 1981) to $\sigma_{\log y} = 0.26$ (McGuire, 1977; Joyner and Boore, 1981). We would expect the overall scatter of ground-motion values in ENA to be in this range.

It is interesting to note the decreasing dependence of PSV on $\boldsymbol{M}$ as oscillator frequency is increased. This is shown by the ξ_1 coefficient of the c_0 parameter in Table 3, which gives the approximate slope of the response, at a small fixed distance, when plotted against moment magnitude. The dependence is very similar to that found by Joyner and Boore (1982) in their preliminary regression analysis of response spectra from WNA.

Figure 5 illustrates the sensitivity of results to the form of the source-scaling model. Both the Brune and Joyner models give similar results for small earthquakes. In the Joyner model, however, the magnitude-dependence decreases for magnitudes greater than the assumed critical magnitude (M_c), as a result of the assumed breakdown in self-similarity when the entire width of the fault plane is ruptured.

TABLE 3

COEFFICIENTS OF PREDICTIVE EQUATIONS

Response Frequency (Hz)		ξ_0	ξ_1	ξ_2	ξ_3
0.2	c_0:	1.743E+00	1.064E+00	−4.293E−02	−5.364E−02
	c_1:	−3.130E−04	1.415E−03	−1.028E−03	
0.5	c_0:	2.141E+00	8.521E−01	−1.670E−01	
	c_1:	−2.504E−04		−2.612E−04	
1.0	c_0:	2.300E+00	6.655E−01	−1.538E−01	
	c_1:	−1.024E−03	−1.144E−04	1.109E−04	
2.0	c_0:	2.317E+00	5.070E−01	−9.317E−02	
	c_1:	−1.683E−03	1.492E−04	1.203E−04	
5.0	c_0:	2.239E+00	3.976E−01	−4.564E−02	
	c_1:	−2.537E−03	5.468E−04	7.091E−05	
10.0	c_0:	2.144E+00	3.617E−01	−3.163E−02	
	c_1:	−3.094E−03	7.640E−04		
20.0	c_0:	2.032E+00	3.438E−01	−2.559E−02	
	c_1:	−3.672E−03	8.956E−04	−4.219E−05	
a_{max}	c_0:	3.763E+00	3.354E−01	−2.473E−02	
	c_1:	−3.885E−03	1.042E−03	−9.169E−05	

The Brune model results assume self-similarity over all magnitudes, and therefore diverge from the Joyner model results above M_c. The value of M_c is not known, but judging from results from WNA, could be as large or larger than 7. If M_c is controlled by the thickness of the seismogenic zone and if, as seems likely, the thickness of the zone is greater in ENA than in WNA, then we would expect M_c to be larger in ENA than in WNA.

A common way of estimating PSV is to multiply peak acceleration and/or peak velocity by appropriate factors and to plot the resulting levels on log–log paper (Newmark and Hall, 1982; most United States and Canadian building codes). When applied to our calculations (Figure 6), this method produces reasonable estimates of PSV for magnitude 5 events but overestimates PSV for larger earthquakes by as much as a factor of 2, for frequencies less than about 10 Hz. For all size events, the method consistently underestimates the high-frequency part of the spectrum, by up to a factor of 3, even though the peak accelerations used in the method were those computed for our ENA ground-motion model. This is in large part due to the much higher frequency content in our theoretical motions (controlled by our choice of f_m = 50 Hz) than exist in the WNA data, from which the amplification factors and faring frequencies published by Newmark and Hall (1982) were derived. The comparison emphasizes the need to predict expected response spectra directly, rather than through the use of standard spectral shapes. Simply put, the frequency content and attenuation of ENA ground motions preclude the use of standard spectral shapes developed empirically from western data. In particular, the enrichment of ENA motions in higher frequencies means that the relationship between maximum ground acceleration and maximum acceleration response is not a simple constant in the frequency range of engineering interest (less than 30 Hz). The acceleration response spectra, S_a, will increase with increasing frequency until frequencies near f_m (50 Hz) are approached.

Model validation. The predictions of the model can be compared with the strong-ground motion and digital-seismograph data base for moderate ($\boldsymbol{M} \sim 5$) ENA earthquakes recorded on competent rock. The theoretical predictions are based on random-process theory; time-domain simulations give essentially the same results. Comparisons are shown in Figure 7 for PSV (5 per cent damping) on rock sites for $f = 2$ and 10 Hz. Comparison has not been made for $a_{\max}$ because the instruments cannot reliably recover frequencies greater than 20 Hz, which will carry $a_{\max}$ in many cases. The data have been scaled to magnitude $\boldsymbol{M}$ = 4.5, using scaling determined from the theory [equation (13)]. Information about the earthquakes used in Figure 7 is included in Table 4. In the case of the ECTN response spectra, horizontal motion has been estimated by multiplying the recorded vertical components by the ratio $H/V = 1.4$ (as in the estimation of m_{Lg}). The actual H/V ratio is a source of scatter in the observations, as it could vary considerably with site conditions, travel path, source characteristics, and frequency of ground motion (Gupta *et al.*, 1983).

The reasonable agreement between the predictions and the calculations support the theoretical model and the specified input parameters. Because of the lack of recent large earthquakes in ENA, there are no ground-motion data against which to check the predictions for large events. However, the demonstrated agreement between theory and data for moderate events in ENA, coupled with the documented success of the method for larger events in the Western United States (Hanks and McGuire, 1981; Boore, 1983; McGuire *et al.*, 1984), provides strong grounds for accepting the model predictions for larger magnitudes. A caveat is that, for suffi-

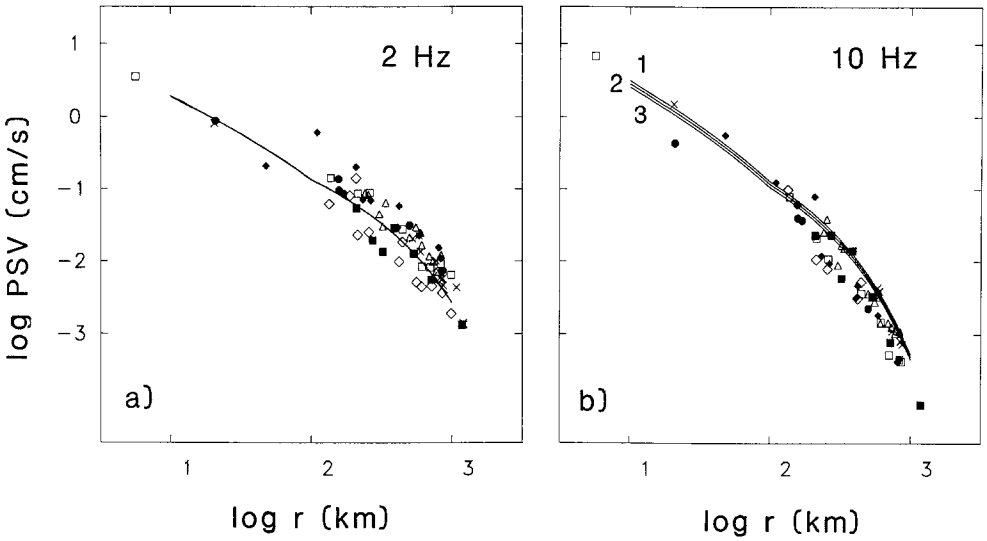

FIG. 7. Comparison of predicted and observed 5 per cent damped pseudo-velocity response spectra (*PSV*) for 2- and 10-Hz oscillators. Predictions given by curves, with r_x = 100 km. Data by symbols: open diamonds = 11 January 1982; filled squares = 19 January 1982; open squares = 31 March 1982; filled diamonds = 16 June 1982; open triangles = 7 October 1983; filled circles = 11 October 1983; X's = 31 January 1986. See Table 4 for source of data. Data have been normalized to a moment magnitude of 4.5, using scaling obtained from the theoretical predictions. Curve 1 uses f_m = 50 Hz; curves 2 and 3 use $\kappa = 1/2\pi f_m$ and $1/\pi f_m$, respectively. The separation between the curves is not distinguishable for the 2 Hz *PSV*.

TABLE 4

EARTHQUAKE DATA

Date	Location	*M*	Source for *M**	Source of Ground-Motion Data*
1 11 82	Miramichi, New Brunswick	5.22	a, b	g
1 19 82	Gaza, New Hampshire	4.36	a, b	g, h
3 31 82	Miramichi, New Brunswick	4.01	b	f, g
6 16 82	Miramichi, New Brunswick	3.90	c	g
10 07 83	Goodnow, New York	5.02	d, b	g
10 11 83	Ottawa, Ontario	3.60	e	g
1 31 86	Painesville, Ohio	4.79	i, j	k

* a = Nguyen and Herrmann (1984); b = J. Boatwright (written communication, 1984); c = Street (1984); d = G. Suarez (written communication to J. Boatwright, 1984); e = fitting ECTN Lg spectra (Boore, unpublished data); f = Weichert *et al.* (1982); g = Atkinson (1985); h = Chang (1983); i = R. Herrmann (oral communication, 1986); j = A. Dziewonski (oral presentation, American Geophysical Union Spring Meeting, 1986); k = Geophysics Division, Geological Survey of Canada, Ottawa, Canada.

ciently large magnitudes, the effects of finite fault rupture may limit near-source ground motions to values lower than those predicted by our model.

Parameter study. Given the unavoidable uncertainty in many of the input parameters describing the generation and propagation processes for earthquakes in ENA, an appreciation of the sensitivity of the predictions is essential. Therefore, parametric analyses have been performed to show the influence of different possible assumptions concerning values of $\Delta\sigma$, β, f_m, and Q in Figures 8 through 11. In each case, the parameters of our standard model were used, with the exception of the variable under consideration. We chose values of the variables that bracket the values in the standard model. If no discernible difference between the results was

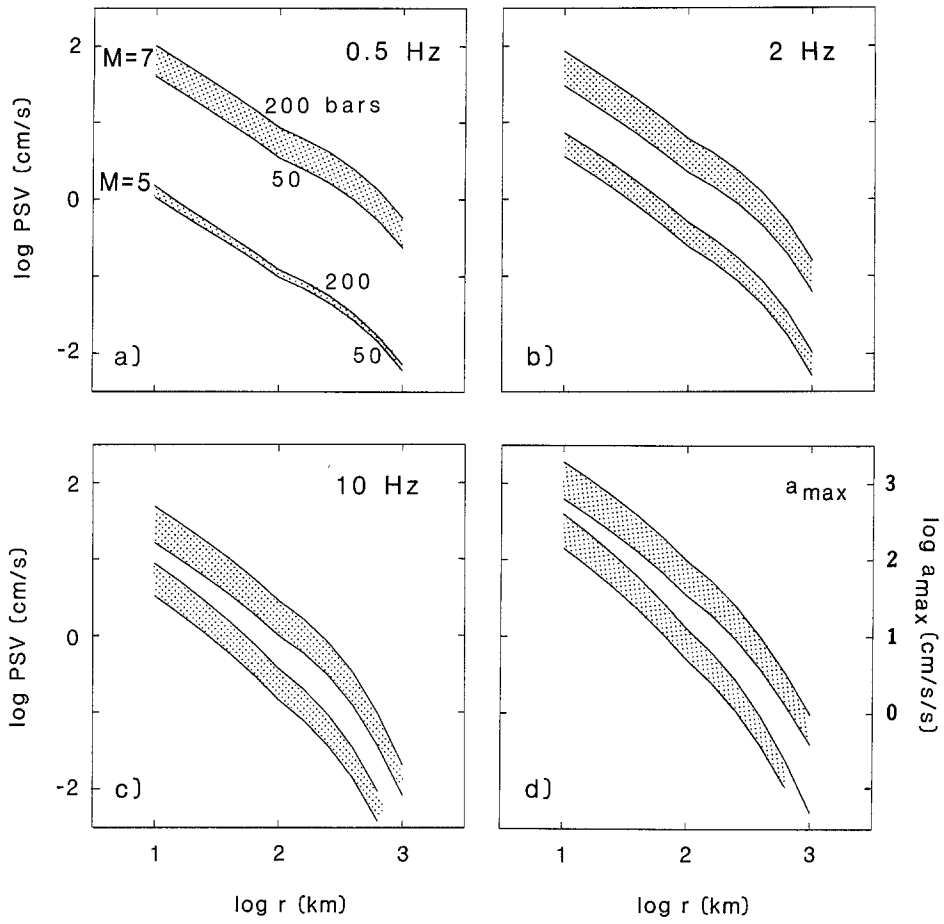

FIG. 8. Dependence of predicted 5 per cent damped pseudo-velocity response spectra (*PSV*), at oscillator frequencies of 0.5, 2, and 10 Hz, and peak ground acceleration (a_p) on stress parameter ($\Delta\sigma$) for two moment magnitudes. The curves defining the lower and upper limits of the *stippled area* used $\Delta\sigma$ = 50 and 200 bars, respectively; the predictions shown in all other figures used $\Delta\sigma$ = 100 bars. r_x = 100 km.

seen when plotted, we did not include the plots here. The dependence of the results on both the type of source-scaling model and the form of the high-frequency filter have already been given in Figures 5 and 7, respectively.

Referring to Figures 8 through 11, the results of the parameter study can be summarized as follows

1. The sensitivity of results to the stress parameter, $\Delta\sigma$, can be significant, especially for larger earthquakes and higher frequency motions (Figure 8). Variations in the stress-parameter are bound to occur, and, to the extent that they cannot be predicted, they will be a source of scatter in observed ground motions.
2. The shear velocity, β, does not have a wide range of values and therefore will not be a source of much variation in the predicted values. For higher frequency motions, the differences are substantially smaller than those shown in Figure 9.
3. The high-frequency cut-off, f_m, is very uncertain in ENA. It could lie anywhere between 30 and 100 Hz and may actually be better expressed as an exponential

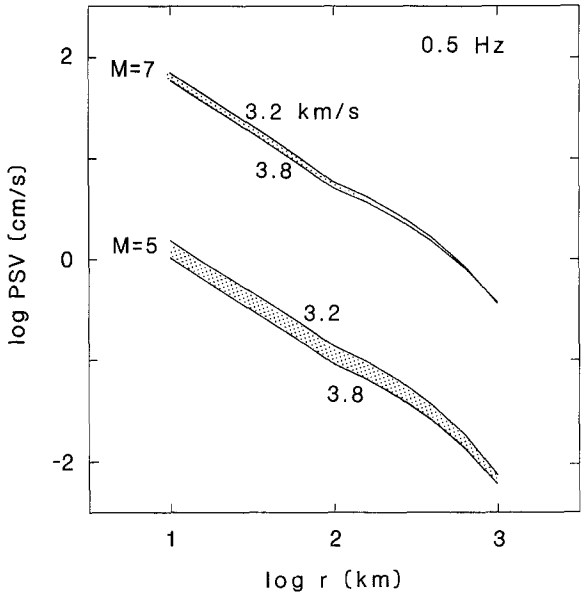

FIG. 9. Dependence of predicted 5 per cent damped pseudo-velocity response spectra (*PSV*), at oscillator frequency of 0.5 Hz, on shear velocity (β) for two moment magnitudes. The curves defining the lower and upper limits of the *stippled area* used β = 3.8 and 3.2 km/sec, respectively; the predictions shown in all other figures used β = 3.5 km/sec. r_x = 100 km. The *PSV* for higher frequency oscillators were less sensitive to β than shown here.

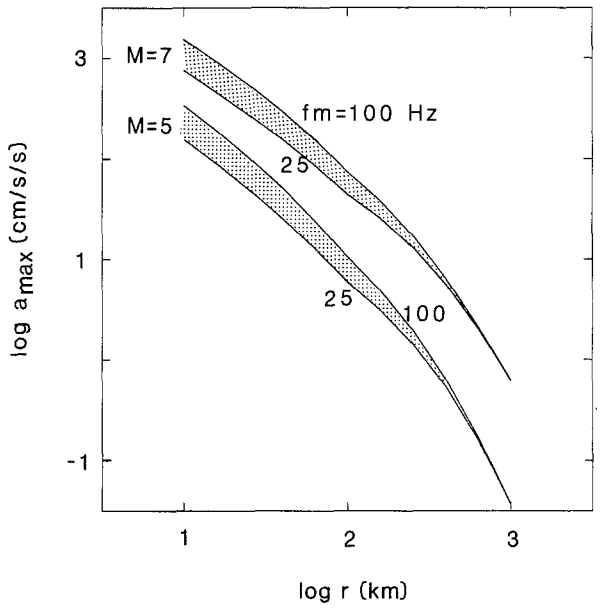

FIG. 10. Dependence of peak ground acceleration (a_p) on high-frequency cut-off (f_m) for two moment magnitudes. The curves defining the lower and upper limits of the *stippled area* used f_m = 25 and 100 Hz, respectively; unless noted, the predictions shown in all other figures used f_m = 50 Hz. r_x = 100 km. Five per cent damped pseudo-velocity response spectra (*PSV*) with frequencies up to 10 Hz showed negligible dependence on f_m for values from 25 to 100 Hz.

decay trend. However, it has no influence on *PSV* for frequencies as high as 10 Hz; it does have an influence on peak acceleration (Figure 10), which has dominant frequencies close to f_m.

4. The Q model has an important effect on motions for sites at large distances (r

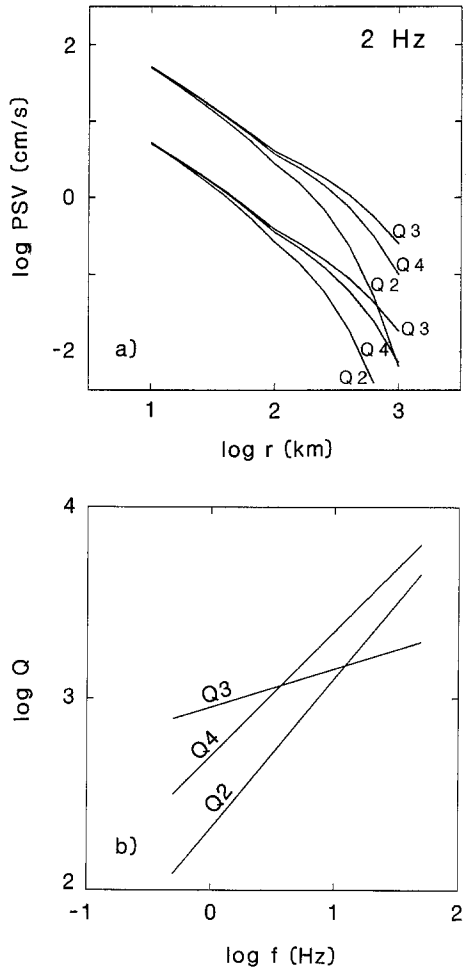

FIG. 11. (a) Dependence of predicted 5 per cent damped pseudo-velocity response spectra (*PSV*), at an oscillator frequency of 2 Hz, on frequency-dependent quality factors (Q) for two moment magnitudes, with $r_x = 100$ km. The Q models, shown in (b), are: $Q2 = 210\,f^{0.78}$; $Q3 = 900\,f^{0.2}$; and $Q4 = 500\,f^{0.65}$. The predictions shown in all other figures used $Q4$. *PSV* for other frequencies show an overall similar dependence on Q.

≧ 100 km) from an earthquake, as shown in Figure 11, and must be accounted for in efforts to reconcile the predictions with historic observations as to felt areas, or with instrumental observations from seismographs at regional distances. From an engineering point of view, however, the choice of the Q function is not very significant; design parameters for important structures are generally geared to resist the potentially destructive effects of moderate to large events occurring relatively nearby (usually less than 100 km).

Parameters for which we have not performed detailed sensitivity studies are the crustal material property ρ, the distance-dependent duration assumption, and possible near-source modifications in effective duration or moment. The largest effects are expected for the near-source modifications and for the duration assumption. For example, if the duration is set to $1/f_0$ rather than $1/f_0 + 0.05r$, then calculations show that the response of a 20 Hz oscillator 100 km from a magnitude 5 earthquake would increase by a factor of 2. (The difference in response is smaller for larger earthquakes and for lower frequency oscillators.)

CONCLUSIONS

A simple theoretical model has been used to develop ground-motion relations for horizontal *PSV* at several frequencies and for a_{max} for hard-rock sites in ENA. The model uses moment magnitude $\boldsymbol{M}$ to describe source size, but the results are readily extended to m_{Lg} by using correlations between magnitude scales determined by the same model. With an assumed constant stress-parameter of 100 bars, the model gives predictions for events of moderate ($\boldsymbol{M} \sim 4.5$) magnitude which are in demonstrable agreement with observations. By contrast, if the stress-parameter is assumed to increase with magnitude as proposed by Nuttli (1983a, b), then the model does not match ground-motion observations. Furthermore, we find no definitive evidence in the magnitude data to suggest a fundamental difference in the scaling of source spectra for earthquakes in ENA and WNA, although the value of the stress-parameter in ENA may be a factor of 2 larger than that in WNA. We therefore conclude that the constant-stress model is likely correct for ENA. However, it is acknowledged that the adequacy of the earthquake source model, particularly for large earthquakes, is the most significant uncertainty in our model.

A major source of uncertainty in applying the theoretical predictions concerns the influence of site effects, which we have not attempted to model. The use of the prediction equations should therefore be restricted to predicting bedrock motions. For areas characterized by soils that may cause significant amplifications (e.g., Mississippi embayment, coastal plain, river valleys), the predicted bedrock motions should serve as input to site-specific soil response models to determine surface ground motions. This approach (or a simple impedance ratio approach) can also be used to predict the influence of soft rock near the surface.

Our results indicate that typical scaling procedures that estimate *PSV* from ground-motion values (a_{max} and v_{max}) may overestimate the expected low-frequency response of rock sites in ENA by a factor of 2 for large events, and furthermore, may underestimate the high-frequency response by an even larger factor. It is therefore essential that estimates of expected response spectra for ENA be made directly, rather than by scaling the acceleration and velocity values.

ACKNOWLEDGMENTS

We have benefited from discussions with Robin McGuire and Gabriel Toro, who have also been developing and applying these techniques to ENA. The encouragment and assistance of our colleagues at the Geological Survey of Canada (formerly Earth Physics Branch) and the U.S. Geological Survey are also greatly appreciated, with particular thanks to Peter Basham and William Joyner. Mary Andrews, Ken Campbell, C. B. Crouse, and William Joyner provided critical reviews that significantly improved the manuscript. The work was partially funded by a grant from the U.S. Nuclear Regulatory Commission.

REFERENCES

Anderson, J. G. and S. E. Hough (1984). A model for the shape of the Fourier amplitude spectrum of acceleration at high frequencies, *Bull. Seism. Soc. Am.* **74**, 1969–1993.

Atkinson, G. M. (1984). Attenuation of strong ground motion in Canada from a random vibrations approach, *Bull. Seism. Soc. Am.* **74**, 2629–2653.

Atkinson, G. M. (1984). Ground motions from moderate earthquakes recorded by the Eastern Canada Telemetered Network, *Geol. Survey Canada, Earth Phys. Branch Open-File No. 85-5*, Ottawa, 76 pp.

Boatwright, J. (1984). Seismic estimates of stress release, *J. Geophys. Res.* **89**, 6961–6968.

Boore, D. M. (1983). Stochastic simulation of high-frequency ground motions based on seismological models of the radiated spectra, *Bull. Seism. Soc. Am.* **73**, 1865–1984.

Boore, D. M. (1986a). Short-period *P*- and *S*-wave radiation from large earthquakes: implications for spectral scaling relations, *Bull. Seism. Soc. Am.* **76**, 43–64.

Boore, D. M. (1986b). The effect of finite bandwidth on seismic scaling relationships, in *Earthquake Source Mechanics*, S. Das, J. Boatwright, and C. Scholz, Editors, Geophysical Monograph 37, American Geophysical Union, Washington, D.C., 275–283.

Boore, D. M. (1987). The prediction of strong ground motion, in *Strong Ground Motion Seismology*, M. Erdik and M. N. Toksöz, Editors, NATO Advanced Studies Institute series, D. Reidel Publishing Company, Dordrecht, The Netherlands (in press).

Boore, D. M. and G. M. Atkinson (1984). Estimation of high-frequency ground moitons east of the Rockies: a preliminary report (abstract), Seismological Society of America, Eastern Section, 54th Annual Meeting, St. Louis, Missouri, October 10–12, 1984, p. 2.

Boore, D. M. and J. Boatwright (1984). Average body-wave radiation coefficients, *Bull. Seism. Soc. Am.* **74,** 1615–1621.

Boore, D. M. and W. B. Joyner (1984). A note on the use of random vibration theory to predict peak amplitudes of transient signals, *Bull. Seism. Soc. Am.* **74,** 2035–2039.

Brune, J. N. (1970). Tectonic stress and the spectra of seismic shear waves from earthquakes, *J. Geophys. Res.* **75,** 4997–5009.

Brune, J. N. (1971). Correction, *J. Geophys. Res.* **76,** 5002.

Campbell, K. W. (1981). Near-source attenuation of peak horizontal acceleration, *Bull. Seism. Soc. Am.* **71,** 2039–2070.

Campbell, K. W. (1982). A preliminary methodology for the regional zonation of peak ground acceleration, *Proc. 3rd Intl. Earthquake Microzonation Conf.*, Seattle, Washington, **1,** 365–376.

Campillo, M., J.-L. Plantet, and M. Bouchon (1985). Frequency-dependent attenuation in the crust beneath central France from *Lg* waves: data analysis and numerical modeling, *Bull. Seism. Soc. Am.* **75,** 1395–1411.

Cartwright, D. E. and M. S. Longuet-Higgins (1956). The statistical distribution of maxima of a random function, *Proc. Roy. Soc. London, Ser. A.* **237,** 212–232.

Chael, E. P. (1987). Spectral scaling of earthquakes in the Miramichi region of New Brunswick, *Bull. Seism. Soc. Am.* **77,** 347–365.

Chang, F. K. (1983). Analysis of strong motion data from the New Hampshire earthquake of 18 January 1982, U.S. Nuclear Regulatory Commission, NUREG/CR-3327.

Choy, G. L., J. Boatwright, J. W. Dewey, and S. A. Sipkin (1983). A teleseismic analysis of the New Brunswick earthquake of January 9, 1982, *J. Geophys. Res.* **88B,** 2199–2212.

Dwyer, J. J., R. B. Herrmann, and O. W. Nuttli (1984). Use of a digital seismic network to study regional *Lg* attenuation and coda *Q* in the central Mississippi Valley, *Earthquake Notes* **55,** 7–8.

Ebel, J. E., P. G. Somerville, and J. D. McIver (1986). A study of the source parameters of some large earthquakes of northeastern North America, *J. Geophys. Res.* **91,** 8231–8247.

Faccioli, E. (1986). A study of strong motions from Italy and Yugoslavia in terms of gross source properties, in *Earthquake Source Mechanics*, S. Das, J. Boatwright, and C. Scholz, Editors, *American Geophysical Union Geophysical Monograph* **37,** 297–309.

Finn, C., C. Carr, and R. B. Herrmann (1986). L_g corner frequencies, seismic moments, and stress drops in the New Madrid seismic zone (abstract), *Earthquake Notes* **57,** 24.

Gupta, I. H., D. H. von Seggern, and R. A. Wagner (1982). A study of variations in the horizontal to vertical *Lg* amplitude ratio in the eastern United States, *Bull. Seism. Soc. Am.* **72,** 2081–2088.

Gupta, I. N., J. A. Burnetti, T. W. McElfresh, D. H. von Seggern, and R. A. Wagner (1983). Lateral variations in attenuation of ground motion in the eastern United States based on propagation of *Lg*, U.S. Nuclear Regulatory Commission, NUREG/CR-3555.

Haar, L. C., C. S. Mueller, J. B. Fletcher, and D. M. Boore (1986). Comments on "Some recent *Lg* phase displacement spectral densities and their implications with respect to the prediction of ground motions in eastern North America" by R. L. Street, *Bull. Seism. Soc. Am.* **76,** 291–295.

Hanks, T. C. (1977). Earthquake stress drops, ambient tectonic stresses and stresses that drive plate motions, *Pure Appl. Geophys.* **115,** 441–458.

Hanks, T. C. (1982). f_{max}, *Bull. Seism. Soc. Am.* **72,** 1867–1879.

Hanks, T. C. and H. Kanamori (1979). A moment magnitude scale, *J. Geophys. Res.* **84,** 2348–2350.

Hanks, T. C. and R. K. McGuire (1981). The character of high-frequency strong ground motion, *Bull. Seism. Soc. Am.* **71,** 2071–2095.

Hasegawa, H. S. (1983). *Lg* spectra of local earthquakes recorded by the Eastern Canada Telemetered Network and spectral scaling, *Bull. Seism. Soc. Am.* **73,** 1041–1061.

Hasegawa, H. S. (1985). Attenuation of *Lg* waves in the Canadian Shield, *Bull. Seism. Soc. Am.* **75,** 1569–1582.

Hasegawa, H. S., P. W. Basham, and M. J. Berry (1981). Attenuation relations for strong seismic ground motion in Canada, *Bull. Seism. Soc. Am.* **71,** 1943–1962.

Herrmann, R. B. (1985). An extension of random vibration theory estimates of strong ground motion to large distances, *Bull. Seism. Soc. Am.* **75,** 1447–1453.

Herrmann, R. B. and A. Kijko (1983). Modeling some empirical vertical component *Lg* relations, *Bull.*

Seism. Soc. Am. **73,** 157–171.

Herrmann, R. B. and O. W. Nuttli (1984). Scaling and attenuation relations for strong ground motion in eastern North America, in *Proc. 8th World Conf. Earthquake Engineering*, Vol. 2, Prentice-Hall, Inc., Englewood Cliffs, New Jersey, 305–309.

Houston, H. and H. Kanamori (1986). Source spectra of great earthquakes: teleseismic constraints on rupture process and strong motion, *Bull. Seism. Soc. Am.* **76,** 19–42.

Irikura, K. and K. Aki (1985). Scaling laws of seismic source spectra and empirical Green function for predicting strong ground motions (abstract), *EOS, Trans. Am. Geophys. Union* **66,** 967.

Joyner, W. B. (1984). A scaling law for the spectra of large earthquakes, *Bull. Seism. Soc. Am.* **74,** 1167–1188.

Joyner, W. B. and D. M. Boore (1981). Peak horizontal acceleration and velocity from strong motion records including records from the 1979 Imperial Valley, California, earthquake, *Bull. Seism. Soc. Am.* **71,** 2011–2083.

Joyner, W. B. and D. M. Boore (1982). Prediction of earthquake response spectra, *U.S. Geol. Surv., Open-File Rept. 82-977*, 16 pp.

Kanamori, H. and D. L. Anderson (1975). Theoretical basis of some empirical relations in seismology, *Bull. Seism. Soc. Am.* **65,** 1073–1095.

Kennett, B. L. N. (1985). On regional *S*, *Bull. Seism. Soc. Am.* **75,** 1077–1086.

Liu, H.-L. and H. Kanamori (1980). Determination of source parameters of mid-plate earthquakes from the waveforms of body waves, *Bull. Seism. Soc. Am.* **70,** 1989–2004.

McGuire, R. K. (1977). Seismic design spectra and mapping procedures using hazard analysis based directed on oscillator response, *Internatl. J. Earthquake Eng. Struct. Dyn.* **5,** 211–324.

McGuire, R. K. (1984). Ground motion estimation in regions with few data, *Proc. 8th World Conf. Earthquake Engineering*, Vol. 2, Prentice-Hall, Inc., Englewood Cliffs, New Jersey, 327–334.

McGuire, R. K., A. M. Becker, and N. C. Donovan (1984). Spectral estimates of seismic shear waves, *Bull. Seism. Soc. Am.* **74,** 1427–1440.

Milne, W. G. and A. G. Davenport (1969). Distribution of earthquake risk in Canada, *Bull. Seism. Soc. Am.* **59,** 729–754.

Mostaghel, N. and G. Ahmadi (1982). Estimation of the peak horizontal ground acceleration based on peak accelerations of the components, *Bull. Seism. Soc. Am.* **72,** 637–642.

Munro, P. S., W. E. Shannon, R. J. Halliday, and D. R. J. Schieman (1985). Canadian Seismograph Operations—1984, *Seismological Series 94*, Earth Physics Branch, Ottawa, Canada.

Nábělek, J. L. (1984). Determination of earthquake source parameters from inversion of body waves, *Ph.D. Thesis*, Massachusetts Institute of Technology, Cambridge, Massachusetts.

Newmark, N. M. and W. J. Hall (1982). *Earthquake Spectra and Design*, Earthquake Engineering Research Institute, 103 pp.

Nguyen, B. V. and R. B. Herrmann (1984). Surface-wave focal mechanisms for some earthquakes in eastern North America (abstract), *EOS, Trans. Am. Geophys. Union* **65,** 240.

Nuttli, O. W. (1973). Seismic wave attenuation and magnitude relations for eastern North America, *J. Geophys. Res.* **78,** 876–885.

Nuttli, O. W. (1979). The relation of sustained maximum ground acceleration and velocity to earthquake intensity and magnitude, U.S. Army Waterways Experiment Station Misc. Paper 5-73-1, Report 16, Vicksburg, Mississippi.

Nuttli, O. W. (1983a). Empirical magnitude and spectral scaling relations for mid-plate and plate-margin earthquakes, *Tectonophysics* **93,** 207–223.

Nuttli, O. W. (1983b). Average seismic source-parameter relations for mid-plate earthquakes, *Bull. Seism. Soc. Am.* **73,** 519–535.

Nuttli, O. W. (1985). Average seismic source-parameter relations for plate-margin earthquakes, *Tectonophysics* **118,** 161–174.

Nuttli, O. W. and R. B. Herrmann (1978). State-of-the-art for assessing earthquake hazards in the United States; credible earthquakes for the central United States, Misc. Paper S-73-1, Report 12, U.S. Army Corps of Engineers, Vicksburg, Mississippi, 100 pp.

Papageorgiou, A. S. and K. Aki (1983). A specific barrier model for the quantitative description of inhomogeneous faulting and the prediction of strong ground motion. Part II. Applications of the model, *Bull. Seism. Soc. Am.* **73,** 953–978.

Shin, T.-C. and R. B. Herrmann (1987). *Lg* attenuation and source studies using 1982 Miramichi data, *Bull. Seism. Soc. Am.* **77,** 384–397.

Somerville, P. G., J. P. McLaren, L. V. LeFevre, R. W. Burger, and D. V. Helmberger (1987). Comparison of source scaling relations of eastern and western North American earthquakes, *Bull. Seism. Soc. Am.* **77,** 322–346.

Street, R. L. (1978). A note on the horizontal to vertical *Lg* wave amplitude ratio in eastern United States, *Earthquake Notes* **49,** 15–20.

Street, R. L. (1984). Some recent *Lg* phase displacement spectral densities and their implications with respect to the prediction of ground motions in eastern North America, *Bull. Seism. Soc. Am.* **74,** 757–762.

Street, R. L. and F. T. Turcotte (1977). A study of northeastern North American spectral moments, magnitudes, and intensities, *Bull. Seism. Soc. Am.* **67,** 599–614.

Street, R. L., R. B. Herrmann, and O. W. Nuttli (1975). Spectral characteristics of the L_g wave generated by central United States earthquakes, *Geophys. J. R. Astr. Soc.* **41,** 51–63.

Weichert, D. H., P. W. Pomeroy, P. S. Munro, and P. N. Mork (1982). Strong motion records from Miramichi, New Brunswick, 1982 aftershocks, *Geol. Survey Canada Earth Phys. Branch Open-File No. 82-34,* Ottawa, Canada.

Wetmiller, R. J., J. Adams, F. M. Anglin, H. S. Hasegawa, and A. E. Stevens (1984). Aftershock sequences of the 1982 Miramichi, New Brunswick, earthquakes, *Bull. Seism. Soc. Am.* **74,** 621–653.

Wu, F. (1984). Studies of July 1981, Cornwall, Canada, and October 7, 1983, Goodnow earthquakes using digital accelerograms (abstract), Seismological Society of American, Eastern Section, 54th Annual Meeting, St. Louis, Missouri, October 10–12, 1984, p. 4.

Yang, J. P. and Y. P. Aggarwal (1981). Seismotectonics of northeastern United States and adjacent Canada, *J. Geophys. Res.* **86,** 4981–4998.

U.S. GEOLOGICAL SURVEY
M.S. 977
MENLO PARK, CALIFORNIA 94025 (D.M.B.)

GEOPHYSICS DIVISION
GEOLOGICAL SURVEY OF CANADA
OTTAWA, ONTARIO, CANADA
K1A 0Y3 (G.M.A.)
CONTRIBUTION NO. 46886

Manuscript received 10 March 1986

APPENDIX

ECTN data. Many of the ground motion data plotted in this report are digital seismograph recordings from the ECTN, which is operated by the Geophysics Division, Geological Survey of Canada (formerly Earth Physics Branch). The data are described in Atkinson (1985). For reference, this Appendix summarizes the procedures for analyzing these ground-motion data.

The ECTN currently consists of 20 short-period vertical seismograph stations located in eastern Canada (most are within a few hundred kilometers of the St. Lawrence River). All stations, with the exception of that at Welcome, Ontario, are founded on rock.

Each station consists of a Geotech S-13 Willmore MK II seismometer, driving a signal amplifier and low-pass filter with a cut-off frequency of 20 Hz (16 Hz for some stations). An A/D converter (9- or 12-bit) is used to digitize the seismic signal 60 times/sec. Digital data are transmitted by UHF ratio and/or telecommunication lines. The minimum detectable ground velocity is 10 nm/sec, while the maximum ground velocity that can be accommodated without overflows is ±320 μm/sec (± 1309 μm/sec for some stations) (Munro *et al.*, 1985). The velocity response of the instrument is approximately constant for frequencies between 2 and 14 Hz (the response is 3 dB down from the maximum at about 1 and 20 Hz).

For each earthquake of interest, the ECTN data have been analyzed to produce a time history of vertical ground acceleration for every station. The analysis procedure is as follows

1. A record length of 68.27 sec, comprised of 4096 samples for the digitization rate of 60 samples/sec, is selected to include the strongest recorded ground shaking. This is generally attributed to the *Lg* phase for distances greater than approximately 70 km.

2. A Fast Fourier Transform converts the (velocity) time series to the corresponding complex data points for frequencies up to 30 Hz.
3. The complex data points are divided by the complex instrument response. Velocity is transformed to acceleration in the frequency domain. For frequencies much outside the flat response range of 1 to 10 Hz, the amplification by the instrument is very low, and the signal becomes indistinguishable from noise. To avoid the attendant errors, the spectrum of the ground motion is truncated at 0.5 Hz, at the low-frequency end, and 20 Hz, at the high-frequency end.
4. The reverse Fast Fourier Transform changes the acceleration spectrum back into the time domain, to provide a ground-motion time history.

The accelerograms are used to calculate response spectra for natural frequencies of 1 to 10 Hz.

The instrument correction procedures employed in these analyses are rather simplified. A truncation (as opposed to a more ideal filter) is applied to the spectra at 0.5 and 20 Hz, and no spectral smoothing is performed. These simplifications are justified by the envisioned use of the data—namely, to provide approximate ground motion and response spectral parameters in the frequency range of 1 to 10 Hz. Since ground-motion time histories of earthquakes of this moderate size, at these large distances, would not be used directly in design analyses, more rigorous instrument correction procedures are not considered necessary.

To test the influence of different possible correction procedures, the following tests were made

1. The effect of window length was tested by considering a double-length (8192 samples) and half-length (1024 samples) windows for intermediate and longer observation distances.
2. The effect of tapering the time signal near the beginning and end of the selected time window was tested for several records.
3. The simple truncation at 0.5 and 20 Hz was compared to a cosine taper beginning at 0.5 and 20 Hz.

None of the above modifications in procedure produced any significant (i.e., more than a few per cent) changes in computed response spectra in the 1- to 10-Hz range.

The signal-to-noise ratio was also checked for the 1- to 10-Hz frequency range. This resulted in the elimination of some of the higher frequency data points at distant stations. Also, at some stations, other arrivals (e.g., *Sn*) act as noise on the *Lg* signal; when these other phases are sufficiently strong they render the *Lg* phase unusable. Some observations were eliminated for this reason. The remaining data are believed to be a good representation of ground-motion levels for moderate ENA earthquakes recorded on rock sites.